Image processing for a more accurate GNSS-based positioning in urban environment

Juliette Marais, Sébastien Ambellouis, Cyril Meurie, Julien Moreau, Amaury Flancquart, Yassine Ruichek

Image processing for a more accurate GNSS-based positioning in urban environment

Juliette Marais[1*], Sébastien Ambellouis[1], Cyril Meurie[1], Julien Moreau[2], Amaury Flancquart[1], Yassine Ruichek[2]
1. IFSTTAR, COSYS, LEOST, 20 rue E. Reclus, BP70317, 59666 Villeneuve d'Ascq, France
+33.3.20.43.84.95, juliette.marais@ifsttar.fr
2. UTBM, SeT, France

Abstract
Most of the Intelligent Transport Systems rely on GNSS positioning information. Unfortunately, most of the vehicles circulate in dense urban areas where the GNSS signals are affected by multipath caused by the buildings surrounding the antenna. The CAPLOC project deals with inaccuracy by associating image processing techniques and signal propagation knowledge to understand and reduce GNSS inaccuracy. Our solution embeds fisheye cameras located on the roof of a vehicle and oriented upwards to capture images of the sky. Our approach consists in processing the images to 1/ determine whether satellites are located in a sky or non-sky region and 2/ construct a 3D model around the camera/antenna in order to estimate the pseudo-range delays caused by the close propagation effects. This knowledge allows us to propose several strategies of exclusion/weighting or correction of these pseudoranges for a better accuracy.

Keywords:
GNSS, Image processing, multipath.

Introduction

The new services of intelligent transports abound. Most of them rely directly or not on position information such as guidance services of course, but also eco-drive systems, "pay as you drive" insurance, speed limit control devices…
Technically, the most-spread solution today relies on the installation of GPS chips on-board of the vehicles, complemented with software and hardware equipment capable of using the position to deliver a service (route calculation, communication system etc.). Indeed, the satellite-based radio navigation system GPS offers the best compromise between cost, simplicity and performance. It can be augmented by the use of the EGNOS signals, for a better accuracy and will be soon compatible with Galileo. Some services, like automotive guidance, are today satisfied with the accuracy obtained. However, if the urban user of a satellite-based positioning system is the most accuracy demander, they suffer from a degraded

service due to the signal propagation conditions, strongly linked to the density of obstacles around the antenna.

The objective of the CAPLOC project (10/2010-01/2015) is to deliver accurate position information, available everywhere, in a context of cost reductions. CAPLOC is a research project. The approach, patented in 2008, is based on the knowledge of the environment of propagation, provided by one or more cameras associated with image processing. The approach is able to detect the satellite signal state of reception and to model the disturbances caused by the surrounding obstacles in order to reduce their impact on GNSS localization. This idea is today adapted in systems embedding 3D numerical maps with similar objectives [1,2]. The CAPLOC system is based on three fisheye cameras installed on the roof of the vehicle as presented on the Figure 1.

Three main axes have been explored in the project, all illustrated with real data:

- Processing of fisheye coloured images recorded in motion to simplify, segment and classify the pixels/regions into three classes: sky, building and vegetation. The goal is the reception state identification of the received satellites [3,17].
- Fisheye stereoscopic perception system associated with a method allowing extracting building structure [4] and their distance to the mobile in order to estimate the delay caused by the signal reflection.
- Use of this knowledge for a more accurate position: by detection and exclusion of the NLOS signal(s); by weighting these signals for a more optimal use of the available data and by correcting the pseudorange estimations thanks to the 3D model. Our method is compared to weighting solutions of the literature [5].

The rest of the paper gives an overview of the realisations for these three main axes.

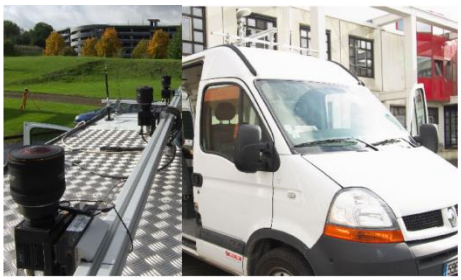

Figure 1: The CAPLOC multi-camera system.

Image processing for satellite state identification

The main objective for satellite state identification is to classify pixels of the acquired image into three classes such as: sky, vegetation and building. Such a classification allows us to obtain several data: the horizon line separating masking obstacles from open sky (with considering or not vegetation as blocked surface), and an evaluation of the size of the sky, vegetation and buildings areas. Figure 2-left shows the synopsis of the global proposed approach where each detection (sky, vegetation and building) which can be made separately permits to increase the robustness of the final detection. In this paper, we consider only the

sky detection that implies that vegetation and building are considered as not-sky. The proposed strategy is also composed of eight steps illustrated in orange and blue colors on Figure 2-left. Once the data (image) acquisition made, the second step consists in transforming the acquired image in a most appropriate color space (which guarantees a better detection/classification of objects of interest). The third step concerns the image filtering with a morphological operator of geodesic reconstruction by dilatation in order to simplify the acquired image. A classification of pixels provided by Fisher's algorithm is also made in order to classify each pixels of the simplified image into two classes (sky and not-sky). But some pixels can be classified incorrectly, that is why, a morphological post-treatment (based on a neighborhood study) which consists in reclassifying incoherent pixels, can be added to enhance the classification. A supplementary step of edge detection is then added to detect the horizon line. The next step consists in satellite repositioning in the acquired and classified images by using an experimental calibration method. Finally, the last step of this strategy consists in identifying which satellite is located in a sky region (received with a direct signal - LOS signal) and in a non- sky region (with blocked/reflected signals – NLOS signal). The proposed strategy of sky/not-sky detection has been evaluated on the CAPLOC database and provides a good classification rate of 97.2 % [3, 16]. Figure 2-middle illustrates an example of the horizon line detection (in green) and Figure 2-right shows a result of sky/not-sky classification (in blue/brown colors) with satellite repositioning.

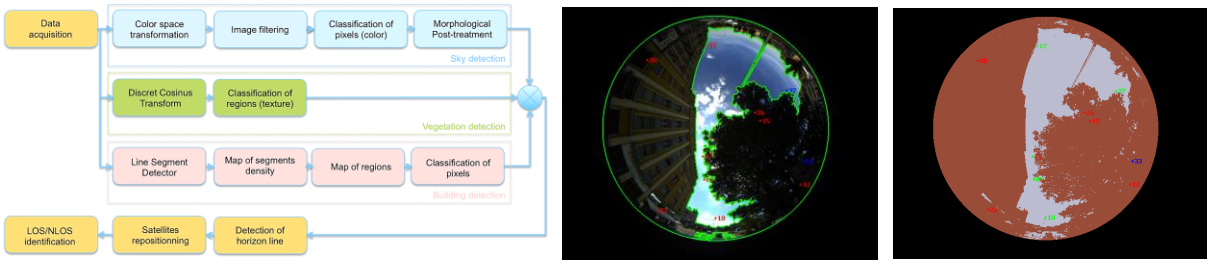

Figure 2: Synopsis of the proposed method for satellites state identification (left), a result of horizon line detection (middle), and sky/not-sky classification result (right)

Fisheye stereoscopic perception system for delay estimation

The delay estimation due to the reflections of the GNSS signals is based on the use of a 3D map of buildings around the antenna. Some works are using commercial 3D maps of cities [2]. In our work, we retrieve the local 3D structure of the buildings surface using a camera system mounted on the roof of the vehicle.

The system is made of two cameras with fisheye lens oriented toward the sky. The 3D structure estimation is obtained thanks to an algorithm that processes each pair of images by following these steps :

1. stereo matching pixels along the epipolar curves using a dynamic programming technique;
2. computation and temporal registration of 3D point clouds;

3. reconstruction of the 3D surfaces.

The rest of this section is dedicated to the description of them. We present some results obtained on real image sequences. To speed up and to improve the accuracy of the 3D point cloud, the calibration of the camera system is required. The calibration is performed at the initialization of the system and is occasionally applied when the vehicle is moving to compensate the vibration effects. The next sub-section deals with this very important step.

The calibration process

The calibration aims at estimating the intrinsic and extrinsic parameters. The intrinsic parameters describe the projection process of the camera (from the meter to the pixel scale). The extrinsic parameters define how to go from the real world to the camera centred reference frames. The CAPLOC system is exploiting three cameras and the parameters have to be computed for all. Much work has been published in the literature on this topic. The most popular technique requires observing a known planar pattern located at different positions and for different orientations [6]. For self-calibration techniques, the knowledge about objects in the scene is not used. These methods consider only correspondences of features points automatically extracted from the images. These techniques have been proposed because of (1) the parameters of the lens (or the combination of lens and mirrors) were partially known and inaccurate and (2) the use of a calibration object or a pattern was impossible. The authors of [7,8] have addressed this topic for omni-directional cameras. In [8], the problem is formalized for a spherical lens projection and more particularly for an equidistant model. We have adapted this method for equisolid model that is fitting better the technical characteristics of the used camera. This algorithm detects and matches some feature points in an image pair and applies a RANSAC/Levenberg-Marquardt based estimation to estimate the parameters. It is detailed in [4] and [8]. The Figure 3 shows the results on a pair of images acquired in Belfort (France). The drawn curves are called epipolar curves. One curve in the left image corresponds to one curve in the right image. Both curves are called conjugate curves and constraint the point cloud calculation. Moreover, they intersect in two epipolar points

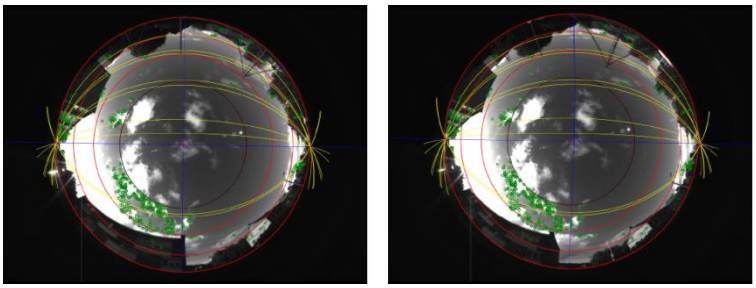

Figure 3: Calibration results on a real pair of images

Point cloud computation

The point clouds are computed by applying a matching algorithm on the pixels lying on two

conjugate curves. We have implemented graph based techniques described in [9,10]. They yield dense map of matched points (p_l, p_r) whose coordinates are used to compute the 3D coordinates of the corresponding point P. The Figure 4 shows one image of the pair, the corresponding distance map and the point cloud obtained.

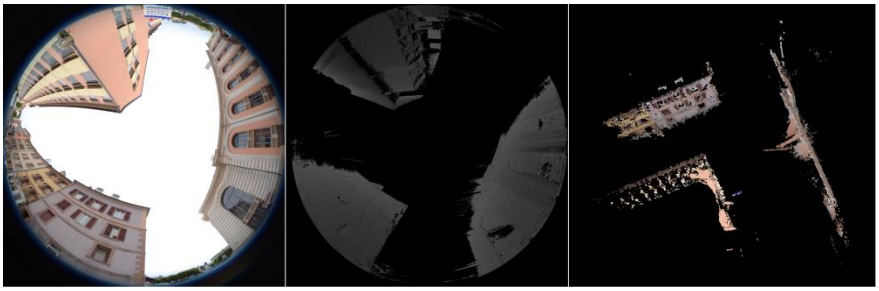

Figure 4: From left to right, the left raw image of a pair, the distance map obtained, and the corresponding point cloud textured with the left image.

One point cloud is estimated locally for each position of the vehicle. A registration method is applied to fuse incrementally the local point clouds calculated along the trajectory of the vehicle. We use an ICP (Iterative Closest Point) based method adapted from the algorithm proposed in [11]: it minimizes iteratively the difference between two consecutive 3D point clouds. The Figure 5 is an illustration of the 3D point cloud obtained after the fusion of the local clouds along a loop path in Belfort.

Building structure approximation

The last step deals with the extraction and the modelling of the frontage of the buildings around the vehicle to finally estimate the pseudo-range delays due to multiple reflections. The frontage of a building is considered as a vertical plane surface. The surface is marked out by the footprint of the building and its height is defined by analysing the distribution of the 3D points above the footprint.

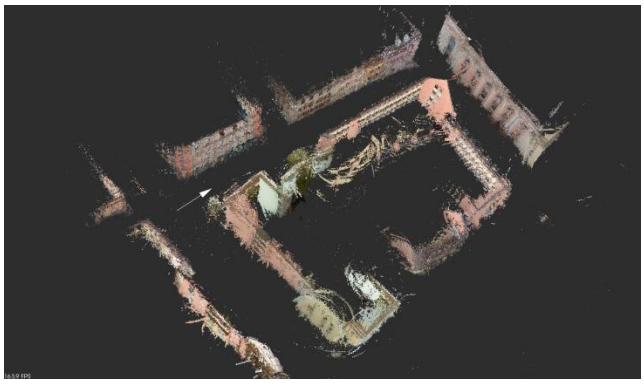

Figure 5: The point cloud obtained by fusing the local map along a loop path in Belfort.

The footprint is estimated by extracting the line segments in the floor projection of the point cloud. We use the Probabilistic Hough Transform proposed in [12]. The Figure 6 shows an

example the footprint it is possible to obtain and the plane fitting results. The two white circles represent the two fisheye cameras. The right camera is located at 4,97m and 13,98m from the line segments of the footprint.

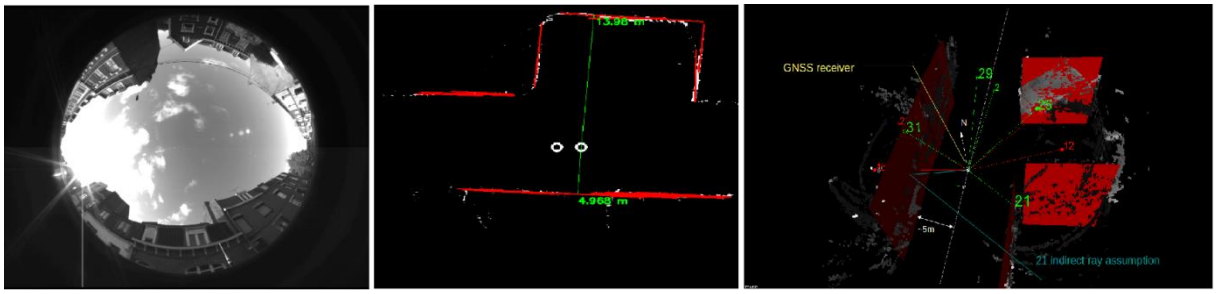

Figure 6: From left to right, a raw image, the extracted footprint of buildings (line segments in red color) and plane fitting result.

Towards a more accurate position

The final use of image in our approach is accuracy enhancement compared to classical use of satellite signals. The objective is to be more accurate than a low cost GNSS receiver, using its pseudoranges. As expressed in the introduction, several kinds of image uses have been tested in the project: the first excludes NLOS signals the position estimation; the second weights NLOS signals in order to limit unavailability and optimize the use of available data; the third is more challenging and aims to estimate delays from the 3D model. The three principles will be describes in the next sub-sections and illustrated with real data in the last section of the paper.

Detection and exclusion of the NLOS signal(s)

One of the multipath mitigation technics consists in excluding the potentially corrupted signals. In our approach, thanks to images, NLOS satellites can be identified and are considered as corrupted satellites because of their delay caused by reflection. As a first assumption, all satellites recognized in a non-sky area are considered as NLOS and excluded from the position computation. Some discussions can be open about the legitimacy of considering vegetation as masking or not, function of the season, their foliage density etc. Their impact has been roughly tested on a test run and let the door open for further work.
Exclusion can be applied in an Extended Kalman Filter (EKF) or a Least Square method.

Weighting these signals for a more optimal use of the available data

Availability is not always guaranteed in urban areas because of the blocking effects of buildings. As exclusion sometimes induces supplementary unavailability, weighting schemes have been tested. The principle is the adding of a weight in a least square solution that reduces the influence of reflected rays without going without this observation. Literature already proposes some weights, based on satellite elevation or carrier-to-noise (CN0) ratio [13,14,15].

Our added-value to these weights is the knowledge of the satellite state of reception. Thus, we have proposed a weight that combines this state, CN0 and elevation. Variance, σ^2, is expressed as:

$$\sigma^2 = k \times \frac{10^{-0.1 \times CN0}}{\sin(\theta)^2}$$

With k function of the satellite state of reception:

$k = 1$ when the satellite is LOS

$k = 2$ when the satellite is NLOS, k being chosen experimentally [16].

Correcting the pseudorange estimations thanks to building structure estimation

As previously mentioned, the urban structure is locally extracted thanks to the stereo sensor and the vehicle can be located relatively to the building frontages. By knowing the North direction projected in the images, it is possible to draw the received satellites in the images (Figure 6) and to conclude if the satellites are LOS or NLOS. Moreover, it is possible to define the number of reflections of an NLOS satellite by applying the following rules to its elevation el:

$$\tan^{-1}\left|\frac{H \times \cos(\alpha)}{2w}\right| < el < \tan^{-1}\left|\frac{H \times \cos(\alpha)}{2\times(L-w)}\right| \Rightarrow 1\ reflection \Rightarrow r_1 = 4 \times w \times \cos(el) \times \cos(\alpha)$$

$$\tan^{-1}\left|\frac{H \times \cos(\alpha)}{2\times(L-w)}\right| < el < \tan^{-1}\left|\frac{H \times \cos(\alpha)}{2\times(L+w)}\right| \Rightarrow 2\ reflections \Rightarrow\ r_2 = 4 \times L \times \cos(el) \times \cos(\alpha)$$

$$el < \tan^{-1}\left|\frac{H \times \cos(\alpha)}{2\times(L+w)}\right| \Rightarrow 3\ reflections \Rightarrow r_3 = 2 \times (2 \times w + L) \times\ \cos(el) \times \cos(\alpha)$$

H, L, w_i and α are defined in the Figure 7 and the r_i values represent the pseudorange delays corresponding to the number of reflections. If we note ρ the pseudorange of the satellite measured by the GNSS receiver, its corrected value is given by $\rho_c = \rho - r_i$.

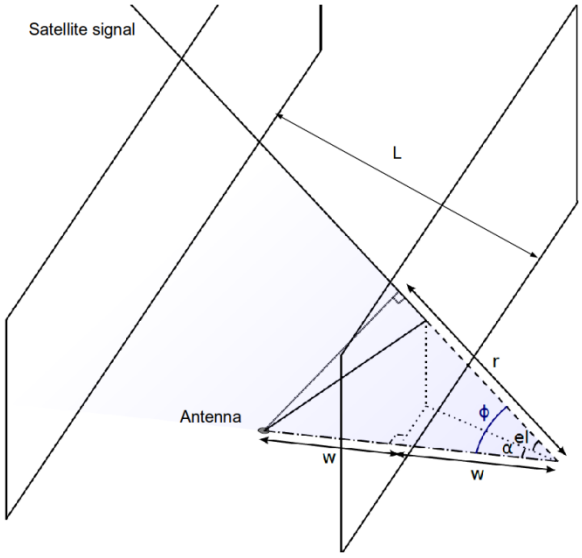

Figure 7: Geometrical principle of the signal delay induced by a reflection in a urban canyon.

Results obtained along a test run in the city of Belfort

The scenarios have been tested with real data. The run is composed of 71 points recorded in the city of Belfort, France. A van has been equipped with a GPS RTK for reference, an uBlox receiver for pseudoranges computations (and navigation message, DOP…), and a camera equipped with a fish-eye lens for image processing. The trajectory is approximately 450m long: the right part is lined with buildings and the left one is bordered by a river. The environment is shown on Figure 8. The frame rate is 25 f/s: 1 f/s is selected to be synchronized with GPS frequency.

Figure 8: Acquisition environment.

The exclusion process applied along this trajectory has shown strong limitations in the second half of the trajectory. Indeed, the unbalanced geometry of the masks induces, with exclusion, a strong degradation of the DOP that degrades performances compared to the use of all satellites. Thus, a compromise has been proposed. It applies exclusion provided that $DOP < 3$).

The results of the exclusion with an EKF are presented as a CDF on Figure 9 with the total exclusion of NLOS satellites (green curve) and with the DOP threshold (pink curve).

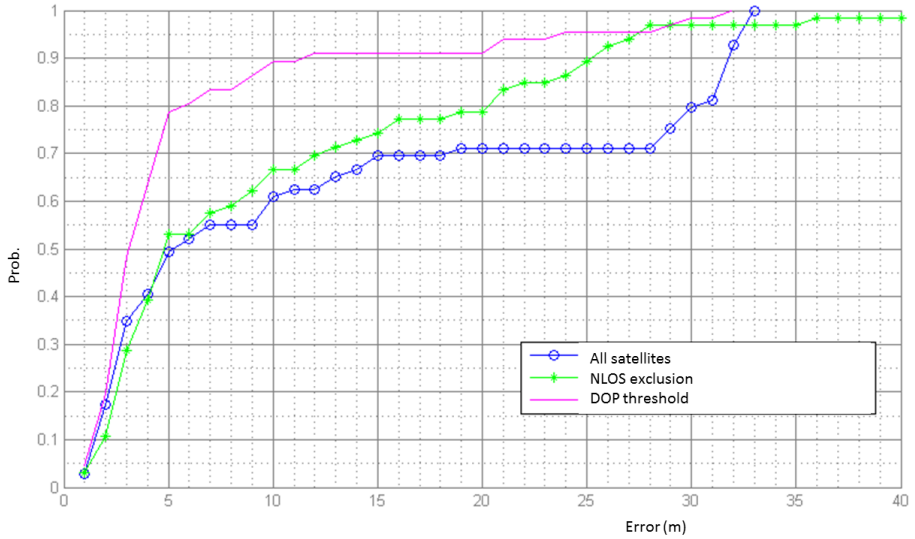

Figure 9: CDF presentation of the accuracy with the exclusion policy.

The weighting schemes applied on the same data set are compared. We illustrate the results of our proposal (in red) compared to the elevation-based weighting scheme of [6] and to the classical EKF solution in Figure 10. In [6], the authors propose a variance equal to: $\sigma^2 = {\sigma_0}/{\sin(\theta)^2}$ with θ, the elevation of the satellite and σ_0, a parameter that depends on the receiver and antenna, chosen equal to 1. More results can be found in [9].

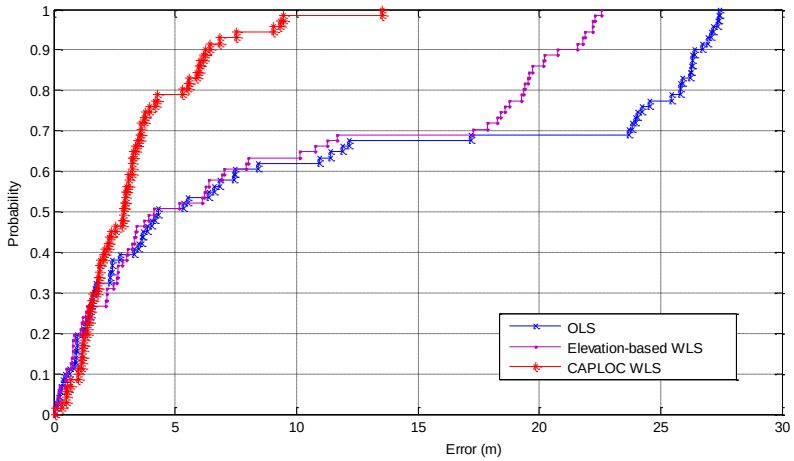

Figure 10: CDF of errors with Ordinary Least Squares (blue curve), Elevation-based weighting Least Square (magenta) and the CAPLOC weighting scheme (red curve).

Table 1 summarizes the performances of the different methods tested. It shows that both methods reduce inaccuracy in this urban environment. The exclusion process reduces the mean error compared to the three state of the art methods tested, but let large errors appears and offers a worse value for the 95th percentile. The weight proposed thanks to the satellite

state determination (CAPLOC WLS) enhance both the mean and the 95th percentile. Indeed, 95% of the positions are more accurate than 9m compared to the 13.5m offered by the Extended Kalman Filter.

Table 1: Comparison of the performances obtained with the different solutions presented above.

	State of the art			Proposals	
	OLS	EKF	El-WLS	NLOS exclusion and DOP threshold	CAPLOC WLS
Mean error	10.57	6.5	8.59	5.73	3.28
95th percentile	27.19	13.53	22.19	23.5	8.98

Preliminary results have been obtained using the 3D approximation of the buildings frontage. The Figure 11 shows the improvement after correcting the measured pseudorange using the rules and the delay equations previously defined. The results for the entire trajectory in Belfort are not completed when we submit this paper. It is presented for one position.

Figure 11: GPS position improvement after pseudorange correction.

Conclusions and perspectives

The final objective of the project was the enhancement of localization accuracy. On the test track located in the city of Belfort, France, we obtain better accuracy (3.28m average with a weighting least square solution) than those given by a “classical least square” method (10.57m) and by exclusion (5.59m). The developed methods still open perspectives of improvement by refining the weighting scheme but also by crossing the a priori knowledge of the satellite state of reception and other dynamic pseudorange estimation algorithms. A task will also be to study the bridges between the use of the 3D embedded models that penetrate the market and our image-based solution.

Image processing activities are also full of perspectives. Industrials of GNSS simulation are interesting in the fisheye based image classification to model the real masking environment of the vehicle and to enrich integrity models in constricted environments. We have adapted the image segmentation approach in an adaptive and non-parametric way the colour and the texture information to yield a fine characterization of the environment

(Sky/building/vegetation). Indeed, a fine segmentation of the image is an added-value for the development of tools for intelligent video surveillance assistance or even diagnosis assistance for health applications and in other applications in other domains of transport, robotics or defense.

To correct the pseudo-range errors due to GNSS signal reflections on buildings has been validated in the literature by embedding Digital Terrain Model (DTM). The accuracy highly depends on the up to date version of the DTM and the accuracy of the initial location to focus on the good area in the model. To tackle the problem of initialization, CAPLOC estimates the 3D structure of the urban environment in real time and position of the mobile relative to its environment. Actually, CAPLOC uses two cameras for the 3D structure estimation. We are adapting the method to a single HD fisheye camera to make the system more compact and easily integrable. The proposed algorithms allow obtaining a fairly accurate 3D model on which it is possible to specify the nature of objects as proposed by the research described above. The single integrated fisheye solution can be used in other context such as that of mobile robotics and especially to develop robots for assistance. Moreover, we aim at operating this system as a part of a drone fleet for terrestrial infrastructure monitoring applications.

The CAPLOC project showed, with upstream research results, that the concept hybridizing dynamic images for knowledge of GNSS signal propagation allowed enhancing localization accuracy in urban environments. Originally developed on public transport operator request, the concept has been mainly validated from road vehicles in CAPLOC, and partially from railway pictures issued from the SATLOC European project. The system developed today consists in a camera equipped with a fisheye lens placed vertically on the top of the vehicle, close to the GNSS antenna, a GNSS receiver and an embedded computer for recording and processing of the data. The system is completely transposable to another transport mode. Future works will have to focus on simplification and miniaturization of the equipment to facilitate the use in any kind of vehicle. The implementation on parallel process to increase processing speed will help to reach the real time, in particular for the 3D model building.

Acknowledgements

The authors want to thank the PREDIT and MEDDE for selecting and funding the project, as well as the CISIT regional program for their support.

References

1. Obst, M., Bauer, S., Wanielik, G. (2012). Urban multipath detection and mitigation with dynamic 3d maps for reliable land vehicle localization. Position Location and Navigation Symposium (PLANS), 2012 *IEEE/ION*, pages 685-691.
2. Peyret, F., Bétaille, D., Piñana-Diaz, C., Toledo Moreo, R., Gomez-Skarmeta, A., & Ortiz, M. (2014). GNSS autonomous localization: Non-Line-Of-Sight satellite detection based

on digital maps of city environments. *IEEE Robotics and Automation magazine*, 21(1).

3. Marais, J., Meurie, C., Attia, D., Ruichek, Y., & Flancquart, A. (2013). Toward accurate localization in guided transport: combining GNSS data and imaging information. *Transportation Research Part C: Emerging Technologies*.
4. Moreau, J., Ambellouis, S., & Ruichek, Y. (2013). Equisolid fisheye stereovision calibration and point cloud computation. *In ISPRS-SS*.
5. Groves, P. D., & Jiang, Z. (2013). Height aiding, C/N 0 weighting and consistency checking for GNSS NLOS and multipath mitigation in Urban areas. *Journal of Navigation*, 66(05), 653-669.
6. Z. Zhang, (2000) A flexible new technique for camera calibration. *IEEE Transactions on Pattern Analysis and Machine Intelligence*, 22(11):1330–1334.
7. C. Geyer and K. Daniilidis, (2022). Paracatadioptric camera calibration, *IEEE Transactions on Pattern Analysis and Machine Intelligence*, 24(5):687–695.
8. Branislav Micusik, (2004) Two-View Geometry of Omnidirectional Cameras, *PhD thesis, Czech Technical University in Prague*.
9. Forstmann, J. Ohya, Y. Kanou, A. Schmitt, and S. Thuering, (2004) Real-time stereo by using dynamic programming, *CVPR*, Washington DC.
10. Y. Boykov and V. Kolmogorov, (2004) An experimental comparison of min-cut/max-flow algorithms for energy minimization in vision, *IEEE Transactions on Pattern Analysis and Machine Intelligence*, pp. 1124–1137.
11. Besl, Paul J.; N.D. McKay (1992), A Method for Registration of 3-D Shapes. *IEEE Trans. on Pattern Analysis and Machine Intelligence*, 14 (2): 239–256.
12. Matas, J., Galambos, C., & Kittler, J. (2000). Robust detection of lines using the progressive probabilistic hough transform. *CVIU*, 78(1), 119-137.
13. Wieser, A., (2007). Weighting GNSS observations and variations of GNSS/INS integration. *Inside GNSS*, 2(1): 26-33.
14. Li, J., Wu, M., (2009). The improvement of positioning accuracy with weighted least square based on SNR. *5th conference on WiCom.* pages 1-4.
15. Tay, S., Marais, J., (2013) Weighting models for GPS Pseudorange observations for land transportation in urban canyons, *6th European Workshop on GNSS Signals and Signal Processing*, December 5-6, Munich.
16. Marais, J., Tay, S., Flancquart, A., Meurie, C., (2015) Weighting with the pre-knowledge of GNSS signal state of reception in urban areas, *European Navigation Conference GNSS*.
17. Attia, D., Meurie, C., Ruichek, Y., Marais, J., (2011) Counting of satellites with direct GNSS signals using Fisheye camera: a comparison of clustering algorithms, *IEEE Intelligent Transportation Systems Conference*, pages 7-12, Washington D.C.